Int. J. Electron. Commun. (AEÜ) 70 (2016) 1235–1240

Contents lists available at ScienceDirect

International Journal of Electronics and Communications (AEÜ)

journal homepage: www.elsevier.com/locate/aeue

Regular paper

Analysis on frequency resolution of EMD based on B-spline interpolation

Yang Yanli [a,*], Deng Jiahao [b]

[a] Tianjin Key Laboratory of Optoelectronic Detection Technology and Systems, Tianjin Polytechnic University, Tianjin, China
[b] School of Mechatronical Engineering, Beijing Institute of Technology, Beijing 100081, China

ARTICLE INFO

Article history:
Received 28 May 2015
Accepted 18 June 2016

Keywords:
Empirical mode decomposition (EMD)
Intrinsic mode function (IMF)
Signal processing
B-spline
Spline filters

ABSTRACT

Empirical mode decomposition (EMD) is an algorithm to split composite signals into narrow subbands termed intrinsic mode functions (IMFs) to obtain a meaningful instantaneous frequency. However, numerical experiments are still the dominant approach adopted to investigate the EMD algorithm. In this paper, the concrete form of IMFs is first discussed. Two simple criteria do not need to count the number of extrema and zero-crossings which are used to define IMFs are presented to identify IMFs. These criteria show that narrow-band signals with non-zero extrema, frequency modulation (FM) signals, and monocomponent signals are all IMFs. The EMD resolution is then analyzed from the digital signal processing perspective. Based on B-spline interpolation, the filtering characteristics of iterative B-spline filters developed to describe IMFs are analyzed. For the first time, a theoretical proof is presented to demonstrate that the EMD method cannot obtain narrow-band IMFs. Nevertheless, a theoretical proof is given to show that the frequency resolution of EMD can be improved in some extent with more sifting iterations.

1. Introduction

In order to obtain a meaningful instantaneous frequency, empirical mode decomposition (EMD) introduced by Huang et al. [1] is designed as an adaptive method to decompose composite signals into narrow subbands. Each subband signal is called an intrinsic mode function (IMF) which represents the oscillation modes imbedded in the data. IMFs need satisfy two conditions [1]: (1) In the whole dataset, the number of extrema and the number of zero-crossings must either equal or differ at most by one, (2) at any point, the mean value of the upper envelope defined by the local maxima and the lower envelope defined by the local minima is zero. A function that only satisfies the condition (1) is called a weak-IMF [2]. IMF based on the local characteristic time scale of signals is the main conceptual innovation for the EMD method.

It is clear from the definition that an IMF can be monocomponent signals or narrow-band signals. If different time scale oscillations are considered as different modes, a composite signal involves more than one oscillatory mode. Separating the different modes into different IMFs is the inherent demand of EMD. It is pointed out in [3] that the instantaneous frequency has meaning only for monocomponent signals, where there is only one frequency or a narrow range of frequencies varying as a function of time. Whether the instantaneous frequency of an IMF extracted by EMD has meaning or not largely depends on the frequency resolution of the EMD method.

As far as the frequency resolution is concerned, EMD cannot separate the components whose frequencies lie within the same octave [4]. Specifically, it has shown that EMD acts as a dyadic filter bank by the numerical experiments with white noise [5] and fractional Gaussian noise [6]. Based on numerical experiments and theoretical analysis on a composite two-tones signal from Fourier domain, Rilling et al. [7] pointed out that the resolution properties of the EMD method is determined by the relationship of amplitude and frequency between different components of signals. Fortunately, the frequency resolution capabilities of EMD can be improved by the masking signal technique [8,9].

Although the EMD method has attracted much attention for its ability of dealing with nonstationary signals, it is still a method based on experience. Numerical experiments are the main ways to investigate the EMD method. There are some problems such as the criterion for judging IMFs need to be resolved for the EMD method. It is pointed out in [10] that the condition (1) involved in definition of IMFs is redundant for some functions, though it does not provide convincing evidences. Moreover, counting the number of zero-crossings of signals will increase the complexity of the EMD algorithm, let alone it is difficult to perform. Hence, it is not the practical method to judge IMFs from the definition.

* Corresponding author.
E-mail address: yyl070805@163.com (Y. Yanli).

http://dx.doi.org/10.1016/j.aeue.2016.06.008
1434-8411/

It is obvious that splines are critical to the EMD method though some improved EMD methods do not use spline interpolation such as the optimization based EMD proposed by Huang et al. [11]. Although the cubic spline interpolation is adopted by Huang et al. [1], it is pointed out in [12] that any polynomial spline can be constructed from a weighted sum of shifted B-splines. From the digital signal processing point of view, the extrema-based EMD sifting process can be regarded as a process of extrema sampling and signal reconstruction [13,14]. Our previous work [15], based on cubic B-spline interpolations, has shown that the process of forming the upper and lower envelopes of signals involves three steps: extrema sampling, interpolation, and filtering by a cubic B-spline filter. Furthermore, a general analytical expression of IMFs extracted by EMD from signals is presented in [15,16]. In this paper, we aim to provide criteria by which to judge IMFs and further analyze the frequency resolution of EMD from the signal processing perspective.

2. The EMD sifting process

As a data-driven method, the EMD algorithm does not have predetermined basis functions. An iteration procedure termed sifting is adopted by EMD to extract IMFs. After decomposed by the EMD algorithm, the signal $x(n)$ can be expressed as [1]

$$x(n) = \sum_{i=1}^{n} c_i(n) + r(n) \tag{1}$$

where $c_i(n)$ denotes an IMF component, and $r(n)$ can be either a monotonic trend or a constant. The process of extracting an IMF by the EMD algorithm can be summarized as follows [1].

A1. Identify all the local extrema of the signal $x(n)$.
A2. Interpolate between maxima by a spline to form the upper envelope $e_{il}^{u}(n)$. Correspondingly, interpolate between minima by a spline to form the lower envelope $e_{il}^{d}(n)$.
A3. Calculate the mean of the upper and lower envelopes $m_{il}(n) = (e_{il}^{u}(n) + e_{il}^{d}(n))/2$.
A4. Compute $h_{il}(n) = x(n) - m_{il}(n)$.
A5. Repeat the above steps until $h_{il}(n)$ is an IMF, then set $c_i(n) = h_{il}(n)$.
A6. Calculate the residue $r_i(n) = x(n) - \sum_i c_i(n)$. Iterate on $r_i(n)$ to obtain the next IMF.

The first four steps of the EMD algorithm are known as one times sifting. Generally speaking, more than one time sifting iterations are needed to extract an IMF. The sifting serves two purposes [1]: to eliminate riding waves, and to make the wave-profiles more symmetric. In order to obtain an IMF, many times sifting iterations sometimes need to be performed. However, too much sifting iterations could make the resulting IMF becomes a pure frequency modulated signal of constant amplitude [1]. Hence, a stopping criterion is needed to limit the sifting times.

The first criterion which is a Cauchy-like criterion is proposed by Huang et al. [1], but it is unrelated to the definition of IMF [17]. Some other methods such as the bandwidth criterion [18], the 3-threshold criterion [19], the energy difference tracking method [20], and partial differential equations based approach [21] are also designed as the stopping criterion. However, there is not a method which is accepted as a popular stopping criterion leading to high efficiency of the EMD algorithm.

3. The concrete form of IMFs

In this section, we provide two simple criteria to identify IMFs by using the original definition of IMFs given by Huang et al. in [1]. These criteria do not need to count the number of extrema and zero-crossings which are used to define IMFs. Here, we consider the continuous functions.

Proposition 1. For a continuous function $x(t)$, if the condition (2) in IMFs definition is satisfied and the upper envelope $e^u(t) > 0$ holds, then $x(t)$ is an IMF.

Proof. The condition (2) in definition IMFs can be expressed as

$$e^u(t) + e^d(t) = 0. \tag{2}$$

For the continuous function $x(t)$, there exists a local minimum between two consecutive local maxima and a local maximum between two adjacent local minima [22]. Then, we consider two consecutive extrema, one maximum $x(t_a)$ and one minimum $x(t_b)$, and suppose that $t_a < t_b$. The upper (resp. lower) envelope is constructed by interpolating between two adjacent local maxima (resp. minima) using a cubic spline in the original EMD algorithm [1]. Thus, we have

$$\begin{cases} e^u(t_a) = x(t_a), \\ e^d(t_b) = x(t_b). \end{cases} \tag{3}$$

Combining with (2), we obtain

$$\begin{aligned} x(t_a) \cdot x(t_b) &= e^u(t_a) \cdot e^d(t_b) \\ &= -e^u(t_a) \cdot e^u(t_b) < 0. \end{aligned} \tag{4}$$

Eq. (4) implies that $x(t)$ at least has one zero-crossing in the interval $[t_a, t_b]$.

With no loss of generality, we suppose that $x(t)$ has two zero-crossings in the interval $[t_a, t_b]$, and let

$$x(t_i) = 0, \quad i = 1, 2, \tag{5}$$

where $t_a < t_1 < t_2 < t_b$. We can be sure that $x(t) \equiv 0$ for any $t \in [t_1, t_2]$. Otherwise, $x(t)$ will at least have one local extremum in $[t_1, t_2]$, which is a contradiction. If we consider $x(t) = 0$ in the interval $[t_1, t_2]$ as one zero-crossing, then we can say that $x(t)$ only has one zero-crossing in $[t_a, t_b]$.

Based on the above analysis, we can conclude that there is only one zero-crossing between any two consecutive extrema if (2) and $e^u(t) > 0$ hold. With this result in hand, we can immediately get that each extremum except the last one is followed by a zero-crossing. Then, it is easy to know that the condition (1) is also satisfied. Hence, Proposition 1 is proved. □

Proposition 2. For a continuous function $x(t)$, if the condition (2) in IMFs definition is satisfied and the value of no local extrema of $x(t)$ is equal to zero, then $x(t)$ is an IMF.

Proof. It is obvious that $e^u(t) \geqslant e^d(t)$. If the condition (2) in IMFs definition is satisfied, we then get

$$\begin{cases} e^u(t) \geqslant 0, \\ e^d(t) \leqslant 0 \end{cases} \tag{6}$$

For two consecutive extrema, one maximum $x(t_a) \neq 0$ and one minimum $x(t_b) \neq 0$, we have

$$\begin{cases} x(t_a) = e^u(t_a) > 0, \\ x(t_b) = e^d(t_b) < 0. \end{cases} \tag{7}$$

Similar to the analysis in the proof of Proposition 1, we can conclude that the condition (1) in IMFs definition is also fulfilled. Therefore, Proposition 2 is established. □

The above two criteria show that the condition (2) in IMFs definition is critical to IMFs. Only the condition (1) in IMFs definition is not enough to define an IMF. A weak-IMF can have dissymmetric

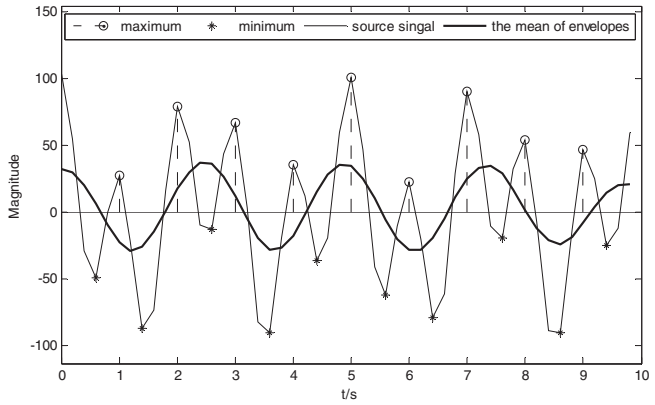

Fig. 1. Illustration a weak-IMF is not an IMF.

upper and lower envelopes. An example shown in Fig. 1 demonstrates that the signal is a weak-IMF but it is not an IMF. Therefore, the aggregate of weak-IMFs is bigger than that of IMFs.

For a narrow-band signal $x(t)$, we can construct the analytic signal

$$s(t) = x(t) + j\hat{x}(t) = |s(t)|e^{j\phi(t)} \tag{8}$$

where $\hat{x}(t)$ denotes the Hilbert transform of the $x(t)$ and $\phi(t) = \arctan(\hat{x}(t)/x(t))$. Then the upper envelope of $x(t)$ can be expressed as

$$e^u(t) = |s(t)| = \sqrt{x^2(t) + \hat{x}^2(t)}. \tag{9}$$

The lower envelope can be written as [10]

$$e^d(t) = -|s(t)|. \tag{10}$$

By Proposition 2, we can conclude that a narrow-band signal with non-zero extrema is an IMF. In addition, by applying Proposition 1, we obtain that monocomponent signals with constant amplitude and frequency modulation (FM) signals are also IMFs. Does EMD can obtain narrow-band IMFs? The answer is presented in next section.

4. Analysis on the EMD resolution

In order to analyze the EMD algorithm from the digital signal processing perspective, we consider digital signals. We first describe IMFs by using a finite order B-spline. Then, we discuss the frequency characteristics of iterative B-spline filters designed to express IMFs. Based on the expression of IMFs, we analyze the frequency resolution of the EMD method from theoretical points of view. It is worthy to mention that these analyses are under the uniform assumption on the extrema.

4.1. Model for IMFs based on finite order B-splines

According to the EMD method, we can get

$$c_i(n) = r_{i-1}(n) - \sum_l m_{il}(n). \tag{11}$$

Moreover, we can know that $m_{il}(n)$ represents the mean of the envelope of $h_{i,l-1}(n)$ if let $h_{i,0}(n) = r_{i-1}(n)$. Let $C_i(e^{j\omega})$ and $R_i(e^{j\omega})$ be the Fourier transform of $c_i(n)$ and $r_i(n)$, respectively. Then, a general analytical expression of IMFs based on B-spline interpolation can be written as [15]

$$C_i(e^{j\omega}) = R_{i-1}(e^{j\omega})Q_{kp}^{L}(e^{j\omega}) - \sum_{l=1}^{L} H_{i,l}^{a}(e^{j\omega})\tilde{Q}_{kp}^{L-l}(e^{j\omega}) \tag{12}$$

where k denotes the order of B-spline, p represents the extrema decimation factor and $h_{i,l}^{a}(n)$ represents the images of $h_{i,l}(n)$. In (12), $Q_{kp}^{l}(e^{j\omega})$ denotes the frequency response of the iterative B-spline filter $q_{kp}^{l}(n)$, and $\tilde{Q}_{kp}^{l}(e^{j\omega})$ denotes the frequency response of the anti-noise B-spline filter $\tilde{q}_{kp}^{l}(n)$.

The expression of $Q_{kp}^{l}(e^{j\omega})$ is written as

$$Q_{kp}^{l}(e^{j\omega}) = [1 - \bar{G}_p^k(e^{j\omega})]^l \tag{13}$$

where $\bar{G}_p^k(e^{j\omega})$ denotes frequency response of the B-spline filter $\bar{g}_p^k(n)$. The expression of $\tilde{Q}_{kp}^{l}(e^{j\omega})$ is written as

$$\tilde{Q}_{kp}^{l}(e^{j\omega}) = Q_{kp}^{l}(e^{j\omega})\bar{G}_p^k(e^{j\omega}). \tag{14}$$

For cubic B-spline interpolation, i.e., $k = 3$, the expression of $\bar{g}_p^3(n)$ is presented in [15]. Here, the expression of B-spline filters for general B-spline interpolation is derived briefly as follows.

Let $\beta^k(t)$ denote the B-spline of order k, and then it can be defined as [12]

$$\beta^k(t) = \underbrace{\beta^0 * \beta^0 * \cdots * \beta^0}_{k+1\text{times}}(t) \tag{15}$$

where the asterisk denotes the convolution operator and [23].

$$\beta^0(t) = \begin{cases} 1, & |t| < 1/2 \\ \frac{1}{2}, & |t| = 1/2 \\ 0, & \text{otherwise.} \end{cases} \tag{16}$$

We can let $b^k(n)$ represent the discrete B-spline and $b_p^k(n) = \beta^k(t/p)|t = n$ denote the discrete B-spline expanded by the factor p. The Fourier transform of $b^k(n)$ is [23]

$$B^k(\omega) = \left[\mathrm{sinc}\left(\frac{\omega}{2\pi}\right)\right]^{k+1}. \tag{17}$$

The discrete signal $x(n)$ up-sampled by an integer p is defined as

$$[x]_{\uparrow p}(n) := \begin{cases} x(n'), & n = pn' \\ 0, & \text{otherwise.} \end{cases} \tag{18}$$

The up-sampled signal $x_p(n)$ can be represented by B-spline as [12]

$$x_p(n) = b_p^k * [x]_{\uparrow p} * [(b_1^k)^{-1}]_{\uparrow p}(n). \tag{19}$$

If let

$$g_p^k(n) = b_p^k * [(b_1^k)^{-1}]_{\uparrow p}(n), \tag{20}$$

then we get

$$x_p(n) = g_p^k * [x]_{\uparrow p}(n). \tag{21}$$

Eq. (21) implies that the B-spline interpolation is equivalent to an interpolator followed by a B-spline filter.

The z-transform of $(b_1^k)^{-1}(n')$ and $b_p^k(n)$ are respectively given by [12,24]

$$(b_1^k)^{-1}(n') \leftrightarrow 1/B_1^k(z), \tag{22}$$

$$B_p^k(z) = \frac{z^{(k+1)(p-1)/2}}{p^k}\left[\frac{1 - z^{-p}}{1 - z^{-1}}\right]^{k+1} B_1^k(z). \tag{23}$$

By applying the Fourier transform on both sides of (20) and deducing with a few simple mathematical manipulations, we find that

$$G_p^k(e^{j\omega}) = \frac{e^{j\omega(k+1)(p-1)/2}}{p^k}\left[\frac{1-e^{-j\omega p}}{1-e^{-j\omega}}\right]^{k+1}\frac{B_1^k(e^{j\omega})}{B_1^k(e^{j\omega p})} = p\left[\frac{\mathrm{sinc}(\frac{p\omega}{2\pi})}{\mathrm{sinc}(\frac{\omega}{2\pi})}\right]^{k+1}\cdot\frac{B_1^k(e^{j\omega})}{B_1^k(e^{j\omega p})} \tag{24}$$

where $sinc(t) = \sin(\pi t)/(\pi t)$ and $G_p^k(e^{j\omega})$ represents the frequency response of $g_p^k(n)$. We can let

$$\bar{G}_p^k(e^{j\omega}) = G_p^k(e^{j\omega})/p. \tag{25}$$

Eq. (12) shows that the IMF $c_i(n)$ can be regarded as equivalent to filtering the residue signal $r_{i-1}(n)$ with an iterative B-spline filter along with some noise. Hence, the characteristics of the iterative B-spline filter help to analyze the frequency resolution of EMD.

4.2. The frequency characteristics of iterative B-spline filters

Theorem 1. For a finite order B-spline, the iterative B-spline filter $Q_{kp}^l(e^{j\omega})$ satisfies

$$|Q_{kp}^l(e^{j\omega})| \to 1,\ \omega \to 2\pi/p. \tag{26}$$

Proof. According to Poisson equation, by using (17), $B^k(e^{j\omega})$ can be rewritten as [25]

$$B^k(e^{j\omega}) = \sum_{n=-[k/2]}^{[k/2]} b^k(n)e^{-jn\omega} = \sum_{n=-\infty}^{\infty}[\mathrm{sinc}(f-n)]^{k+1}. \tag{27}$$

Then, we have

$$B^k(e^{jp\omega}) = \sum_{n=-\infty}^{\infty}[\mathrm{sinc}(pf-n)]^{k+1}. \tag{28}$$

It is obvious that $sinc(f-n) = (-1)^n\sin(\pi f)/(\pi f - \pi n)$ [25]. By using (24), $Q_{kp}^l(e^{j\omega})$ can be rewritten as

$$\begin{aligned} Q_{kp}^l(e^{j\omega}) &= [1-\bar{G}_p^k(e^{j\omega})]^l \\ &= \left\{1-\left[\frac{\mathrm{sinc}(pf)}{\mathrm{sinc}(f)}\right]^{k+1}\cdot\frac{B_1^k(e^{j\omega})}{B_1^k(e^{j\omega p})}\right\}^l \\ &= \left[1-\left[\frac{\sin(\pi pf)}{p\sin(\pi f)}\right]^{k+1}\frac{\sum_{n=-\infty}^{\infty}\left[\frac{(-1)^n\sin(\pi f)}{(\pi f-\pi n)}\right]^{k+1}}{\sum_{n=-\infty}^{\infty}\left[\frac{(-1)^n\sin(\pi pf)}{(\pi pf-\pi n)}\right]^{k+1}}\right]^l \\ &= \left[1-\left[\frac{1}{p}\right]^{k+1}\frac{\sum_{n=-\infty}^{\infty}\left[\frac{(-1)^n}{(f-n)}\right]^{k+1}}{\sum_{n=-\infty}^{\infty}\left[\frac{(-1)^n}{(pf-n)}\right]^{k+1}}\right]^l \\ &= \left[1-\frac{1+\sum_{n=-\infty}^{-1}\left[\frac{(-1)^n}{1-n/f}\right]^{k+1}+\sum_{n=1}^{\infty}\left[\frac{(-1)^n}{1-n/f}\right]^{k+1}}{1+\sum_{n=-\infty}^{-1}\left[\frac{(-1)^n}{1-n/pf}\right]^{k+1}+\sum_{n=1}^{\infty}\left[\frac{(-1)^n}{1-n/pf}\right]^{k+1}}\right]^l \end{aligned} \tag{29}$$

where $f = \omega/(2\pi)$. If we let

$$u^k(f) = \begin{cases} \sum_{n=1}^{\infty}\left(\frac{1}{\left(1-\frac{n}{f}\right)^{k+1}}+\frac{1}{\left(1+\frac{n}{f}\right)^{k+1}}\right), & k \text{ odd} \\ \sum_{n=1}^{\infty}(-1)^{k+1}\left(\frac{1}{\left(1-\frac{n}{f}\right)^{k+1}}+\frac{1}{\left(1+\frac{n}{f}\right)^{k+1}}\right), & k \text{ even} \end{cases}, \tag{30}$$

then we have

$$Q_{kp}^l(e^{j\omega}) = \left[1-\frac{1+u^k(f)}{1+u^k(pf)}\right]^l = \left[\frac{1-u^k(f)/u^k(pf)}{1+1/u^k(pf)}\right]^l. \tag{31}$$

From (30), we can find

$$\begin{cases} \frac{1}{(1-n/f)^{k+1}}+\frac{1}{(1+n/f)^{k+1}} > 0, & k \text{ odd} \\ \frac{1}{(1-n/f)^{k+1}}+\frac{1}{(1+n/f)^{k+1}} \\ = \frac{(-f)^{k+1}}{(n-f)^{k+1}}+\frac{f^{k+1}}{(n+f)^{k+1}} < 0. & k \text{ even} \end{cases} \tag{32}$$

Then, we get

$$u^k(f) > 0,\quad f \in (0,1). \tag{33}$$

Hence, we have

$$1/u^k(pf) > 0,\quad f \in (0,1/p). \tag{34}$$

It is proved in [25] that

$$|u^k(f)| < \frac{4}{(1/f-1)^{k+1}},\quad f \in (0,1). \tag{35}$$

According to (30), we have,

$$1/u^k(pf) \to 0,\quad f \to 1/p \tag{36}$$

and

$$u^k(f) < \frac{4}{(p-1)^{k+1}},\quad f \to 1/p \tag{37}$$

By combining (31), (36) and (37), we get that the iterative B-spline filter $Q_{kp}^l(e^{j\omega})$ converges to 1 as ω tends to $2\pi/p$, which brings the desired result. □

Theorem 2. For a finite order B-spline, when $l \to \infty$, the iterative B-spline filter $Q_{kp}^l(e^{j\omega})$ satisfies

$$\lim_{l\to\infty} Q_{kp}^l(e^{j\omega}) = \begin{cases} 1, & \omega = 2\pi/p \\ 0, & \omega \in (0, 2\pi/p) \end{cases}. \tag{38}$$

Proof. The expression of $Q_{kp}^l(e^{j\omega})$ is shown in (31). By using (33), we have

$$u^k(f) > -1,\quad f \in (0,1). \tag{39}$$

Combining (33) with (34) gives

$$\frac{-u^k(f)}{u^k(pf)} < \frac{1}{u^k(pf)},\quad f \in (0,1/p). \tag{40}$$

From (40), we find that

$$1-\frac{u^k(f)}{u^k(pf)} < 1+\frac{1}{u^k(pf)},\quad f \in (0,1/p). \tag{41}$$

We then get

$$|Q_{kp}^l(e^{j\omega})| < 1,\quad \omega \in (0, 2\pi/p). \tag{42}$$

Hence, combining (33) with Theorem 1, we get the desired result described by (38). □

Theorem 1 and Theorem 2 show that $Q_{kp}^l(e^{j\omega})$ $\omega \in (0, 2\pi/p]$ have a good frequency selectivity when $l \to \infty$. Using the non-ideal low-pass characteristics of the finite order B-spline filter, the iterative B-spline filter $Q_{kp}^l(e^{j\omega})$ can obtain a better filtering performance. Theorem 2 implies that the EMD method can obtain very

narrow oscillation mode functions. Does it is really true? This problem can be answered through analyzing the frequency resolution of EMD.

4.3. Frequency resolution of EMD

Theorem 1 implies that the amplitude-frequency characteristics of iterative B-spline filters are affected by the sifting times. Therefore, for the spline with finite order, the frequency resolution of EMD is not only determined by the extrema rate, but also affected by the sifting times.

However, the noise generated in the sifting process will influence the frequency resolution of EMD. The second term in (12) represents new components in the IMF subbands. It is already reported in [26] that EMD sifting process will generate new frequency components. Moreover, it is pointed out in [15] that the reason caused new components in IMF subbands is the sub-Nyquist extrema sampling and the cubic B-spline filter which is far from an ideal low-pass filter.

In fact, the IMF subbands do not contain noise in some special cases. A special case is the extrema decimation factor equals to 2 [15]. In most cases, the frequency resolution of EMD is affected by the characteristics of iterative B-spline filters and anti-noise B-spline filters.

Based on (12), the process of extracting an IMF by EMD can be depicted by Fig. 2. It is shown in [15] the noise generated in the EMD sifting process can be suppressed by the mean of envelopes. Hence, $h^a_{i,l}(n)$ is the noise remained after reducing the mean of the envelopes from signals. It cannot be denied that the new components have a little influence to the EMD results in most cases. Otherwise, the EMD cannot be used to many applications.

In fact, it is difficult to trace new components in the EMD sifting. Here, we only consider a simple case assumes that $h^a_{i,l}(n)$ is the same for each sifting times. Then, the IMF expressed by (12) can be rewritten as

$$\begin{aligned} C_i(e^{j\omega}) &= R_{i-1}(e^{j\omega})\ Q^L_{kp}(e^{j\omega}) - H^a_i(e^{j\omega})\sum_{l=1}^{L}\tilde{Q}^{L-l}_{kp}(e^{j\omega}) \\ &= R_{i-1}(e^{j\omega})Q^L_{kp}(e^{j\omega}) - H^a_i(e^{j\omega})\hat{Q}^L_{kp}(e^{j\omega}) \end{aligned} \tag{43}$$

where

$$\hat{Q}^L_{kp}(e^{j\omega}) = \sum_{l=1}^{L}\tilde{Q}^{L-l}_{kp}(e^{j\omega}) = \sum_{l=1}^{L}\left[1-\bar{G}^k_p(e^{j\omega})\right]^{L-l}\bar{G}^k_p(e^{j\omega}). \tag{44}$$

It is clear from (43) that $\hat{Q}^L_{kp}(e^{j\omega})$ is used to remove noise which generates in the course of extracting IMFs. So, $\hat{Q}^L_{kp}(e^{j\omega})$ is called the IMF anti-noise filter. The IMF anti-noise filter cannot remove low frequency noise because $\hat{Q}^1_{kp}(e^{j\omega}) = \bar{G}^k_p(e^{j\omega})$ is a low pass filter.

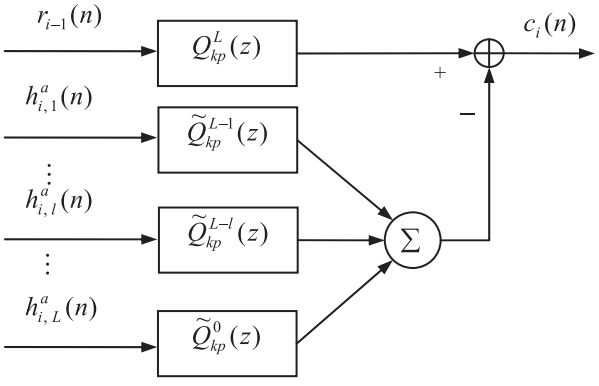

Fig. 2. Schematic illustration of extracting an IMF by the EMD algorithm for $p > 2$.

It is obvious that

$$\begin{aligned} Q^L_{kp}(e^{j\omega}) + \hat{Q}^L_{kp}(e^{j\omega}) &= [1-\bar{G}^k_p(e^{j\omega})]^L \\ &\quad + \sum_{l=1}^{L}[1-\bar{G}^k_p(e^{j\omega})]^{L-l}\bar{G}^k_p(e^{j\omega}) = 1. \end{aligned} \tag{45}$$

Eq. (45) shows that the amplitude characteristics of iterative B-spline filters and IMF anti-noise filters are complementary. Hence, the IMF extracted by EMD in the case of $p > 2$ is not a narrow-band signal. A simple example is shown in Fig. 3. The EMD results shown in Fig. 3 are obtained from a multi-component signal with white Gaussian noise by using the masking signal technology in the case of $p = 4$ and 1000 times sifting iterations. It is obvious from Fig. 3 that it does not have a stop band in IMF $c_1(n)$ and it only has a little high frequency component in the residue $r_1(n)$.

The frequency responses of IMF anti-noise filters are shown in Fig. 4. It is shown in Fig. 4 that the anti-noise ability of IMF anti-noise filters decreases with more sifting iterations. The IMF anti-noise filter becomes band stop filters from low-pass filters as the sifting times increasing for $p = 3$. Moreover, it has a pass band in the high frequency band as the sifting times increasing for $p = 4$ and $p = 5$. This is the reason that the IMF subband shown in Fig. 3 has some noise in high frequency band.

It is reported in [7] that EMD can decompose a two-tones signal correctly when the extrema rate is equal to the frequency of the high-frequency component and it is twice greater than the frequency of the low-frequency component. Nevertheless, Fig. 4 implies that baseband images still can introduce new components, as demonstrated in Fig. 5. Therefore, the second term in (12) must equal to zero to guarantee that the IMF subband does not have new components. It is difficult to extract IMF without new components only relying on the EMD algorithm. We only can say that the frequency resolution of EMD can be improved with more sifting iterations in some extent. The anti-noise ability of the EMD algorithm decreases with increasing the sifting times. The noise generated in sifting process causes EMD cannot obtain narrow-band IMFs.

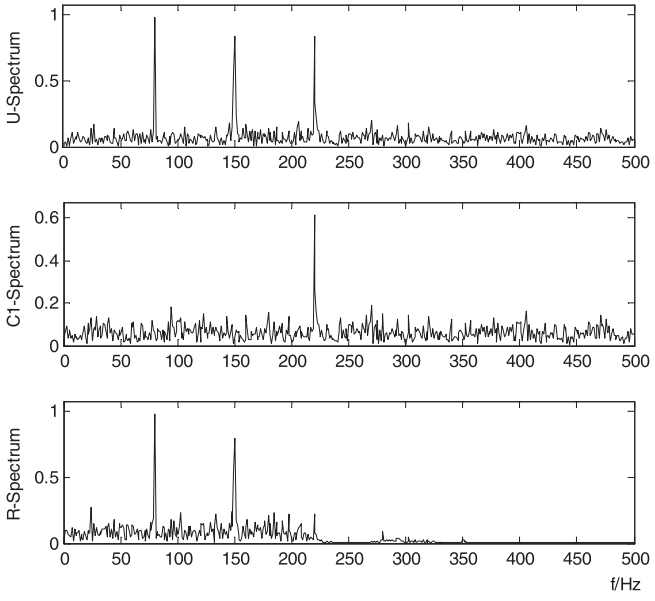

Fig. 3. Illustration of the IMF extracted by EMD from a signal with white Gaussian noise. The top panel is the spectrum of the original signal (U). The middle panel is the spectrum of the IMF (C1). The bottom panel is the spectrum of the residue (R).

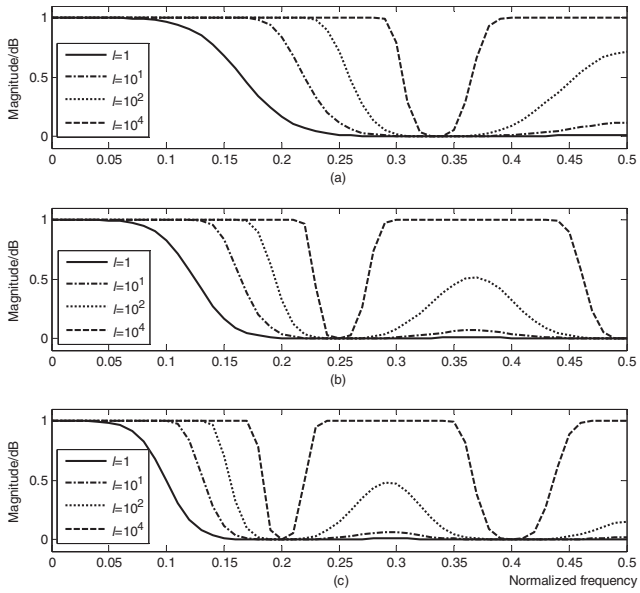

Fig. 4. Magnitude response of IMF anti-noise filters with respect to frequency while varying the sifting times. (a) $p = 3$. (b) $p = 4$. (c) $p = 5$.

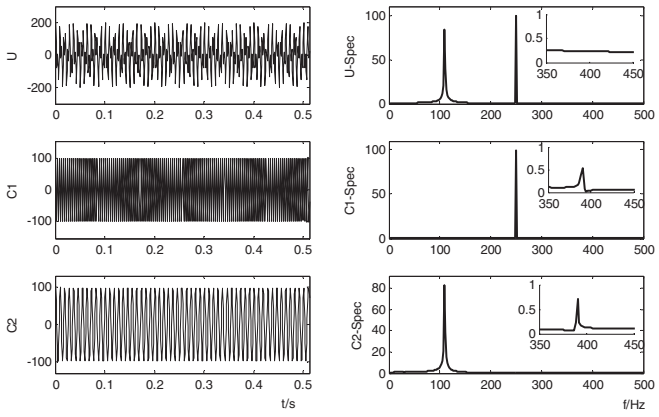

Fig. 5. Illustration of new components caused by baseband images. The left top panel is the original signal (U) and the bottom is the IMFs (C1 and C2). The right panels are the spectrum of the left corresponding panel. Each IMF is obtained by sifting 1000 times.

5. Conclusion

We have proposed two practical criteria to identify IMFs based on the definition. One criterion is only based on the envelopes of signals and the other is associated with the envelopes and extrema of signals. These criteria provide a proof for the EMD sifting stopping criterion which does not count the number of the zero-crossings and extrema of signals. By using these criteria, we deduce that narrow-band signals with non-zero extrema, FM signals, and monocomponent signals are all IMFs.

We have further analyzed the frequency resolution of EMD from a digital signal processing perspective based on the B-spline interpolation. We have shown that the filtering characteristics of iterative B-spline filters have been improved as increasing iterations. Based on analysis on the characteristics of iterative B-spline filters, we have proved theoretically that the frequency resolution of EMD can be improved with more sifting times without considering the influence of noise generated in the EMD sifting process. We have then shown that the noise generated in the course of extracting IMFs will affect the frequency resolution of EMD. The EMD method cannot obtain narrow-band IMFs considering the influence of noise. More sifting iteration only can in some extent to improve the frequency resolution of EMD. In the practical application, it needs to limit the excessive EMD sifting iterations.

Acknowledgments

This work was supported in part by National Natural Science Foundation of China (NSFC) No. 61401305, and Natural Science Foundation of Tianjin, China No. 15JCYBJC16500.

References

[1] Huang NE, Shen Z, Long SR, Wu ML, et al. The empirical mode decomposition and Hilbert spectrum for nonlinear and non-stationary time series analysis. Proc R Soc Lond A 1998;454:903–95.
[2] Vatchev V, Sharpley R. Decomposition of functions into pairs of intrinsic mode functions. Proc R Soc Lond A 2008;464:2265–80.
[3] Boashash B. Estimating and interpreting the instantaneous frequency of a signal—Part 1: fundamentals. Proc IEEE 1992;80(4):520–38.
[4] Senroy N, Suryanarayanan S. Two techniques to enhance empirical mode decomposition for power quality applications. In: Presented at Proc. IEEE Power Eng. Society General Meeting, Tampa, Florida.
[5] Wu ZH, Huang NE. A study of the characteristics of white noise using the empirical mode decomposition method. Proc R Soc Lond A 2004;11(2):112–4.
[6] Flandrin P, Rilling G, Goncalvés P. Empirical mode decomposition as a filter bank. IEEE Signal Process Lett 2004;11(2):112–4.
[7] Rilling G, Flandrin P. One or two frequencies? The empirical mode decomposition answers. IEEE Trans Signal Process 2008;56(1):85–95.
[8] Deering R, Kaiser JF. The use of a masking signal to improve empirical mode decomposition. In: Proc. IEEE Int. Conf. Acoust., Speech Signal Process. (ICASSP). p. 485–8.
[9] Laila DS, Messina AR, Pal BC. A refined Hilbert–Huang transform with applications to interarea oscillation monitoring. IEEE Trans Power Syst 2009;24(2):610–20.
[10] Feldman M. Theoretical analysis and comparison of the Hilbert transform decomposition methods. Mech Syst Signal Process 2008;22(3):509–19.
[11] Huang BQ, Kunoth A. An optimization based empirical mode decomposition scheme. J Comput Appl Math 2013;240:174–83.
[12] Unser M, Aldroubi A, Eden M. B-spline signal processing: Part I—Theory. IEEE Trans Signal Process 1993;41(2):821–33.
[13] Yang YL, Deng JH, Tang WC, et al. Nonuniform extrema resampling and empirical mode decomposition. Chin J Electron 2009;18(4):759–62.
[14] Yang YL. Theoretical analysis and application investigation of empirical mode decomposition [Ph.D. dissertation]. Beijing, China: Sch. of Mech. Eng., Beijing Inst. of Technol.; 2010.
[15] Yang YL, Miao CY, Deng JH. An analytical expression of empirical mode decomposition based on B-spline interpolation. Circuits Syst Signal Process 2013;32(6):2899–914.
[16] Yang YL. Empirical mode decomposition as a time-varying multirate signal processing system. Mech Syst Signal Process 2016;76–77:759–70.
[17] Huang NE, Wu ML, Long SR, Shen SSP, Qu WD, Gloersen P, Fan KL. A confidence limit for the empirical mode decomposition and Hilbert spectral analysis. Proc Roy Soc Lond A 2003;459:2317–45.
[18] Xuan B, Xie QW, Peng SL. EMD sifting based on bandwidth. IEEE Signal Process Lett 2007;14(8):537–40.
[19] Rilling G, Flandrin P, Gonçalvès P. On empirical mode decomposition and its algorithms. In: Presented at the IEEE EURASIP Workshop Nonlinear Signal Image Processing, Grado, Italy.
[20] Cheng JS, Yu D, Yang Y. Research on the intrinsic mode function (IMF) criterion in EMD method. Mech Syst Signal Process 2006;20(4):817–24.
[21] Diop EHS, Alexandre R, Boudraa AO. Analysis of intrinsic mode functions: a PDE approach. IEEE Signal Process Lett 2010;17(4):398–401.
[22] Li J, Gray RM. Context-based multiscale classification of document images using wavelet coefficient distributions. IEEE Trans Image Process 2000;9(9):1604–16.
[23] Unser M. Splines: a perfect fit for signal and image processing. IEEE Signal Process Mag 1999;16(6):22–38.
[24] Unser M, Aldroubi A, Eden M. Fast B-spline transforms for continuous image representation and interpolation. IEEE Trans Patt Anal Machine Intell 1991;13:277–85.
[25] Unser M, Aldroubi A, Eden M. Polynomial spline signal approximations: filter design and asymptotic equivalence with Shannon's sampling theorem. IEEE Trans Inf Theory 1992;38(1):95–103.
[26] Bouzid A, Ellouze N. Maximum error in discrete EMD decomposition of periodic signals. In: Proc. 15th Int. Conf. Digital Signal Process. (DSP). p. 563–6.